REVIEW OF COMPTON SCATTERING PROJECTS

A. D'Angelo, INFN Roma II, Via della Ricerca Scientifica,1 I-00133 Rome, Italy

Abstract

The backward scattering of Laser light against high energy electrons may be used to produce highly polarized photon beams of low background, with an energy resolution of few percent. The general characteristics of Compton backscattering beams are outlined and the application of this technique to different electron accelerators is reviewed. The results from existing facilities are presented with an outlook to planned future installations.

1 INTRODUCTION

In 1963 R. Milburn [1] and F.R. Arutyunian and V.A. Tumanian [2] pointed out for the first time that the Compton scattering of Laser light against high energy electrons could produce γ-ray beams. In the following five years this idea was developed in several laboratories [3, 4, 5, 6], where low intensity photon beams were obtained. In 1978 the first γ-ray *facility* based on Compton backscattering technique, the LADON beam, started to work in Frascati [7, 8, 9, 34]. It was produced by the interaction of the electrons accumulated in the storage ring Adone with the high intensity photons available *inside* a Laser cavity; the outcoming flux was useful for the study of photonuclear reactions.

Today the technique is well established [11]: several working facilities exist, that make use of commercial Lasers on electron storage rings to produce highly polarized photons in the energy range useful for Nuclear physics (from 100 MeV to 1800 MeV) and other projects will become operational in the next few years. The main characteristics of most of the existing projects are shown in Table 1.

In the next sections we will enter into the details of the experimental technique and we will show how the use of a Free Electron Laser (FEL) as photon source offers a very promising possibility both to extend the energy spectrum down to the X-ray region [40] and to obtain a relevant increase of the useful photon flux.

2 THE COMPTON BACKSCATTERING TECHNIQUE

2.1 Kinematics and energy spectum

If a Laser photon of energy k_1 strikes a relativistic electron of energy E with a relative angle $\theta_1 = 180°$, it is scattered in the backward direction inside a narrow cone with the axis coinciding with the incoming electron beam. If θ and θ_2 are the values of the photon scattering angle with respect to the incoming electron and photon beams respectively, the energy of the final photon k is

$$k = k_1 \frac{1 - \beta cos\theta_1}{1 - \beta cos\theta + \frac{k_1}{E}(1 - cos\theta_2)} \qquad (1)$$

where β is the electron velocity in units of light speed c. If we consider relativistic electron sources, the following approximations hold:
$\gamma = E/m >> 1$, $\beta \simeq 1$, $\theta_1 \simeq \theta_2 \simeq 180°$ and $\theta << 1$;
relation (1) may then be rewritten as follows, neglecting the very week dependence upon θ_1

$$k = E\frac{z}{1 + z + x} \qquad (2)$$

where $z = 4\frac{Ek_1}{m^2}$ and $x = (\theta\gamma)^2$. For a fixed Laser line and electron beam energy, the maximum scattered photon energy k_{max} (Compton edge) is obtained at $\theta = 0$ and it is given by the following relation

$$k_{max} = E\frac{z}{1 + z} = \frac{4}{m^2}\,\frac{E^2\,k_1}{(1 + z)}. \qquad (3)$$

The dependence of k_{max} upon the electron energy E is nearly quadratic and it is shown in Figure 1 for different commercial Laser lines and electron beam energies ranging from 10 MeV to 10 GeV. It is interesting to note that the outcoming photon energy spans from the X-ray energy region, useful for solid state physics applications, up to to the Multi-GeV energy region, for nuclear and particle physics investigation.

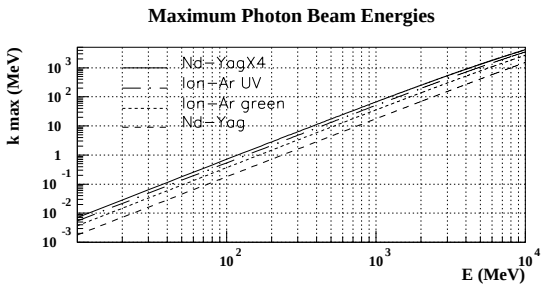

Figure 1: Values of the maximum photon energy as a function of the electron energy E for different Laser lines.

If a FEL is used, the incoming Laser energy is given by the relation

$$k_1 = \frac{chk_w\gamma^2}{\pi(1 + a_w^2)} \qquad (4)$$

Table 1: General characteristics of Compton backscattering facilities for Nuclear physics

Project Name	Electron Energy (GeV)	Laser Energy (eV)	Photon Energy (MeV)	Energy Resolut. (MeV)	Electron Current (A)	Beam Intensity $(\frac{KHz}{MeV})$	Operat. Date
LADON [7, 9, 10]	1.5	2.45	$35-80$	$2-4$	0.05	2	1978-93
ROKK-1 [12]	1.8-5.5	$2.34-2.41$	$100-960$	2	0.01	0.2	1982-85
LEGS [13]	2.5	$2.41-3.53$	$110-330$	5	0.2	33	1987
ROKK-2 [14, 15]	0.35-2	$2.41-3.53$	$30-220$	4	0.2	9	1987
ROKK-1M	2	$1.17-4.68$	$100-1600$	$10-20$	0.1	3	1993
GRAAL [16, 17]	6	$2.41-3.53$	$400-1500$	16	0.15	6	1995
SPRING-8	8	$2.41-4.68$	≤ 3000	2	$0.1-0.2$	1	1998
TJNAF [18]	6	2.41	≤ 1100	1	$1.6\,10^{-6}$	50	2000
HIGS [30, 31, 39]	1	2-12.5	≤ 220	0.8	0.1	10^4	1996
ELFE [32]	$15-30$	$2.41-3.52$	$3-20\,10^3$	≥ 16	$0.05-0.15$	$0.1-1$	-

where k_w is the undulator wave number and a_w is the normalized rms vector potential of the undulator. The value of k_1 may usually be tuned by changing a_w and obtaining a continuous variation of the maximum available photon energy.

It is useful to define the following quantities

$$a = \frac{1}{1+z} \tag{5}$$

$$\rho = \frac{k}{k_{max}} = \frac{1}{1+ax}; \quad (0 < \rho \leq 1) \tag{6}$$

$$\chi = \frac{\rho^2(1-a)^2}{1-\rho(1-a)}; \quad (0 < \chi \leq \frac{(1-a)^2}{a}) \tag{7}$$

$$cos\alpha = \frac{1-\rho(1+a)}{1-\rho(1-a)}; \quad (-1 \leq cos\alpha \leq 1). \tag{8}$$

The total energy spectrum of the outcoming photon beam is proportional to the differential cross section for Compton scattering in the laboratory frame, which may be expressed as a function of the scattered photon energy by means of the relation

$$\frac{d\sigma}{dk} = \frac{2\pi r_e^2 a}{k_{max}}(1+\chi+cos^2\alpha) \tag{9}$$

where $r_e = 2.818$ fm is the classical radius of the electron. Curves of the cross section are shown in Figure 2 in the case of the UV line of an Ion-Ar Laser impinging on electrons of energies $E = 6.05$ GeV (as it is the case of the Graal beam) and 30 GeV, respectively.

The total energy spectrum is slowly varying with the photon energy. Comparing it to Bremsstrahlung beams it does not present the low energy divergence and the rate of accidental events coming from the low energy part of the spectrum is strongly reduced. This property makes backscattering Compton γ-ray beams preferable when the reaction under investigation requires a clean rejection of background events.

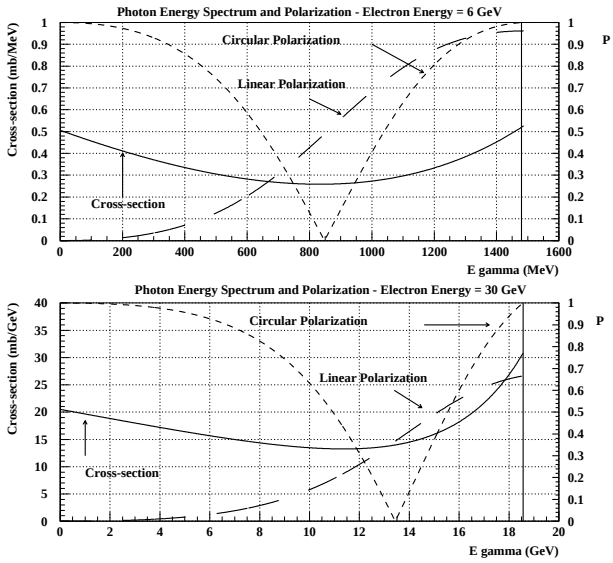

Figure 2: Energy spectrum and beam polarization for incoming electron beam energy $E = 6.04$ GeV (Upper figure) and $E = 30.$ GeV (Lower figure) for a Laser energy $k_1 = 3.53$ eV.

2.2 *Energy resolution*

Using the correlation between the energy of the emitted photon and its scattering angle θ it is possible to select the highest part of the energy spectrum collimating the scattered photon beam. If $\Delta\theta$ is the half aperture of the collimator, the fractional energy resolution $\Delta k/k_{max}$ of the collimated beam is given by

$$\frac{\Delta k}{k_{max}} = \frac{k_{max}-k}{k_{max}} = \frac{x_c}{1+z+x_c} \tag{10}$$

where $x_c = (\gamma\Delta\theta)^2$.

Collimation may be used as an energy defining method only if $x_c \ll 1$, which usually requires that $E < 1$ GeV

and that the angular divergence of the incoming electron beam (defined as σ'_x) satisfies the relation $\sigma'_x \ll 1/\gamma$.

In the case of incoming electron beam energies in the multi-GeV region, it is necessary to use a tagging technique to obtain an energy resolution for the γ-ray beam of the order of few per cents. Collimation may still be used to remove the untagged low energy part of the spectrum, so that only tagged high energy photons would impinge on the target and accidental events would be reduced.

The collimation technique is also used in the case of very high photon fluxes, such as those expected when a FEL is used, because the rate of accidental coincidences prevents from obtaining a clear analysys of the tagging information.

Two tagging techniques have been used in existing facilities, namely *internal* and *external*. In the first case the scattered electrons are deflected from the main orbit by the magnetic lattice of the storage ring, used as a momentum analyzer. Detecting the electron horizontal displacement from the main orbit at a selected location of the storage ring, it is possible to infer the scattered photon energy.

In the case of an external tagging the scattered electrons are removed from the main orbit by a bending magnet, are momentum analyzed by an external spectrometer and their energies are deduced by detecting their position in the magnetic focal plane.

Both techniques may reach the lowest energy resolution limit on the photon beam imposed by the electron beam characteristics. In the case of internal tagging, the position sensitive detectors may be located closer to the electrons main orbit and a wider range of tagged photon energies is obtained. The tagging detectors however must have high spatial resolution ($\delta x < 1$ mm) and are exposed to high fluxes of synchrotron radiation. On the other hand external tagging systems are more expensive to build and operate but the tagging detectors are usually easier to access and may be built of plastic scintillators, as high spatial resolution is not required.

3 INTENSITY

The photom beam flux may be expressed as follows in terms of the Compton differential cross section, reported in (9), and of the spatial densities of the electron and Laser beams u_e and u_γ

$$\frac{d\dot{n_\gamma}}{dk} = c(1+\beta)\frac{d\sigma}{dk}\int u_e\, u_\gamma\, dV. \qquad (11)$$

The electron spatial density for a stored beam is

$$u_e(x,y,z) = \frac{I}{c\,e}\frac{1}{2\pi\sigma_x\sigma_y} exp[-(\frac{x^2}{2\sigma_x^2}+\frac{y^2}{2\sigma_y^2})] \qquad (12)$$

where I is the electron current, $\sigma_x = \sigma_x(z)$ and $\sigma_y = \sigma_y(z)$ are the horizontal and the vertical dispersions of the electron beam depending on the electron longitudinal position. The Laser photon spatial density is

$$u_\gamma(x,y,z) = \frac{P}{ck_1}\frac{1}{\omega^2} exp(-2\frac{x^2+y^2}{\omega^2}) \qquad (13)$$

where P is the laser power and $\omega = \omega(z)$ is the transversal dimension of the Laser beam

$$\omega(z) = \omega_0^2\left[1+\frac{(z-z_0)^2}{b^2}\right] = \omega_0^2\left[1+\left(\frac{z-z_0}{\omega_0}\frac{\lambda}{\pi}\right)^2\right]. \qquad (14)$$

Here λ and ω_0 are the wavelength and the waist of the Laser beam. After space and energy integration of (11), the total γ-ray flux is equal to

$$\dot{n_\gamma} = P\; I\; L \qquad (15)$$

where the luminosity L is

$$L = \frac{2\sigma}{\pi c k_1 e}\int \frac{dz}{\sqrt{\omega^2+4\sigma_x^2}\sqrt{\omega^2+4\sigma_y^2}}. \qquad (16)$$

Typical values for L are in the range $L \simeq 10^7\ A^{-1}W^{-1}s^{-1}$. Using commercial Laser powers ($P \simeq 5-10$ W) on electron beams circulating in storage rings ($I \simeq 0.1-0.2$ A) it is possible to obtain total photon fluxes of $10^7\ \gamma/s$.

Linear accelerators or extracted electron beams are characterized by lower electron currents and require more powerful photon sources.

3.1 Laser systems

The Laser power P is the only parameter that could be increased to obtain higher photon fluxes. In a conventional Laser system the optical resonator is made of two mirrors located at the two ends of the tube containing the active medium. The useful Laser power, extracted from the optical cavity, is [33]

$$P = P_i\frac{T}{L_i+T} \qquad (17)$$

where L_i is the internal cavity power loss and $T = -ln(r_1 r_2)$ is the coupling factor of the two mirrors having reflectivities $|r_1|^2$ and $|r_2|^2$, respectively. The value of T is optimized by the constructor to maximize the output power, however P is usually only few per cent of the internal stimulated power P_i. The Laser optic characteristics are fixed by the mirrors geometry and an additional system of lenses may be used to focus the extracted Laser power on the electron-Laser interaction region. The described set-up is being used at the LEGS and GRAAL facilities. It is not difficult to operate and provides stable photon fluxes, well above the limit normally imposed in storage ring facilities for the reduction of the electron beam lifetime.

An alternative solution is to use the internal Laser power P_i by constructing an optical resonator that *includes* the interaction region. The optical cavity is made of two high reflectivity mirrors that are located several meters apart and must be carefully aligned to maximize the useful power. This idea was applied to the LADON facility, where powers up to $P_i = 80$ W were obtained. However the reflectivity of

the mirrors suffered deterioration due to radiation damage and the average useful power was lower.

The external Laser power P may also be amplified by two orders of magnitude using a resonant optical cavity. This possibility is extensively discussed in the proposal for the construction of a Compton backscattering γ-ray beam at the TJNAF Laboratory (ref. [18]).

Very high fluxes may be obtained using a FEL as in the HIGS facility at the Duke University [30, 31, 39] and the intracavity Compton backscattering beams obtained on the CLIO [35] and the UVSOR [36] FELs. This solution is more expensive and complicated and requires a dedicated electron accelerator. The FEL process is shown in the first three frames of Figure 3. The optical cavity lenght is optimized in order to synchronize the photon and the electron bunches. When the electrons and the photons travel in the same direction the electrons radiate as they pass the undulator and also produce stimulated radiation of the same frequency of the photons stored in the optical cavity. When the Laser pulses reflect on the mirror and reenter the undulator they strike the following incoming electron bunch producing photons by means of Compton scattering, as shown in the last three frames of Figure 3.

4 POLARIZATION

The degree of polarization (P_γ) of the scattered photons is proportional to that of the Laser beam

$$\text{Lin. Pol.} \quad P_\gamma = P_{Laser} \frac{(1 - cos\alpha)^2}{2\,(\chi + 1 + cos\alpha^2)} \tag{18}$$

$$\text{Circ. Pol.} \quad P_\gamma = P_{Laser} \left| \frac{(2+\chi)\, cos\alpha}{(\chi + 1 + cos\alpha^2)} \right| \tag{19}$$

where χ and $cos\alpha$ are defined in (7) and (8). Curves of linear and circular polarization are reported in Figure 2 as a function of the photon energy in the case $k_1 = 3.53\ eV$ (the UV line of an Ar-Ion Laser) for incoming electron energies $E = 6.06$ and 30 GeV, respectively. The degree of polarization is maximum at the Compton edge, where the spin-flip amplitude for highly relativistic electrons vanishes and the scattered photons almost retain the initial Laser polarization. In the case of circular polarization the photons scatter with opposite elicity in the backward hemisphere [34] and retain the total degree of polarization at $k = k_{max}$, where

$$\rho = 1 \quad cos\alpha = -1 \quad \chi = \frac{(1-a)^2}{a} \tag{20}$$

so that

$$\text{Circular Polarization} \quad P_{\gamma\ max} = P_{Laser}. \tag{21}$$

In the case of linear polarization there is a drop of the maximum degree of transferred polarization when the electrons are in the multi-GeV region

$$\text{Linear Polarization} \quad P_{\gamma\ max} = P_{Laser} \frac{2}{2+\chi}. \tag{22}$$

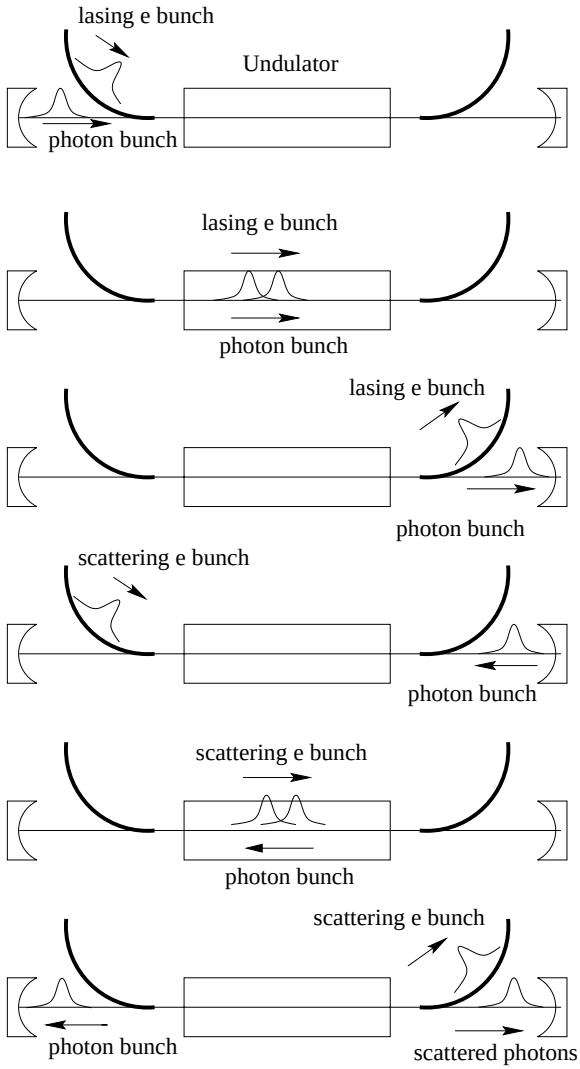

Figure 3: Intracavity FEL production process and Compton backscattering [30].

However changing the Laser line it is possible to keep the degree of linear polarization above $P = 50\%$ for a wide photon energy range.

5 BACKGROUND

The main background is due to high energy photons produced by the electron Bremsstrahlung on the atoms of the residual gas in the vacuum chamber of the storage ring. The rate of these events may be calculated knowing the electron current and the vacuum pressure [11] and it results only of the order of 1% of the Compton beam intensity in the tagged energy range.

A different source of background is due to the low energy X-rays produced by synchrotron radiation; this rays are not able to induce nuclear reactions on the target but may cause damage to the experimental set-up, especially on the optical components and to any detector located close

to the vacuum chamber.

When collimated, almost all the γ-rays hitting the target are tagged and highly polarized. Compared to Bremsstrahlung the Compton Backscattering beams are therefore very clean facilities.

6 CONCLUSIONS

The Compton technique is well established in several laboratories and provides highly polarized photon beams of good energy resolution and very low background. The advent of the FEL technique enables the production of very high fluxes and tunable maximum energies both in the X-ray and the γ-ray energy ranges. We would like to conclude recalling that the clean features of these beams are very appealing also for medical applications such as radiosurgery and radiation terapy [37, 38].

7 REFERENCES

[1] R. H. Milburn, Phys. Rev. Lett. **10** (1963) 75.

[2] F. R. Arutyunyan and V. A, Tumanian, Phys. Lett. **4** (1963) 176.

[3] O.F. Kulivov et al. Phys. Lett. **13** (1964) 344.

[4] C. Bemporad et al. Phys. Rev. B **138** (1965) 1546.

[5] J. Ballam et al. Phys. Rev. Lett. **23** (1969) 498.

[6] V. Bayer ans V. A. Khoze Sov. J. Nucl. Phys. **2** (1969) 238.

[7] L. Casano et al. Laser and Unconv. Opt. J. **55** (1975) 3.

[8] G. Matone et al. Lect. Notes Phys., **62** (1977) 3.

[9] L. Federici et al. Nuovo Cimento B **59** (1980) 247.

[10] D. Babusci et al. Nucl. Instr. & Meth.**A 305** (1991) 19.

[11] D. Babusci et al. Rivista Nuovo Cimento **19** (1996) 1.

[12] A.A. Kazakov et al. JETP Lett. **40** (1984) 445.

[13] A. M. Sandorfi et al. IEEE Trans. **NS-30** (1983) B3093.

[14] G. Ya. Kezerashvili et al. Novosibirsk Preprint **91-118** (1991).

[15] G. Ya. Kezerashvili et al. Nucl. Instr. & Meth. **A328** (1993) 506.

[16] D. Babusci et al. Nuovo Cimento **103 A** (1990) 11.

[17] J. P. Bocquet et al. Proc. of the XIII Int. Conf. on Particles and Nuclei, Perugia 1993, Books of Abstr. 835.

[18] B. E. Norum and T. P. Welch, "An Intense Polarized Photon Source at CEBAF Hall B", (1993).

[19] T. Scott Carman et al, "Production of Gamma-Rays for Nuclear Physics Using the Duke Free-Electron-Laser Facility, Technical Report, TUNL, (1994).

[20] T. Scott Carman et al. Nucl. Instr. & Meth. **A 378** (1996) 1.

[21] A. D'Angelo et al. Nucl. Phys. **A 622** (1997) 226c.

[22] A. Yariv Quantum Electronics, Jonh Wiley & Sons, 187.

[23] D. Babusci et al. Phys. Lett B **355** (1995) 1.

[24] F. Glotin et al. Nucl. Instr. & Meth **A393** (1997) 519.

[25] M. Hosaka et al. Nucl. Instr. & Meth **A393** (1997) 525.

[26] B. Girolami et al. Phys. Med. Bio. **41** (1996) 1581.

[27] K.J. Weeks, Nucl. Instr. & Meth. **A393** (1997) 544.

[28] V.N. Litvinenko et al. Phys. Rev. Lett. **24** (1997) 4569.

[29] A. Luccio and A.B. Brik, "An Intense Polarized Photon Source at CEBAF Hall B", (1993).

[30] T. Scott Carman et al, "Production of Gamma-Rays for Nuclear Physics Using the Duke Free-Electron-Laser Facility, Technical Report, TUNL, (1994).

[31] T. Scott Carman et al. Nucl. Instr. & Meth. **A 378** (1996) 1.

[32] A. D'Angelo et al. Nucl. Phys. **A 622** (1997) 226c.

[33] A. Yariv Quantum Electronics, Jonh Wiley & Sons, 187.

[34] D. Babusci et al. Phys. Lett B **355** (1995) 1.

[35] F. Glotin et al. Nucl. Instr. & Meth **A393** (1997) 519.

[36] M. Hosaka et al. Nucl. Instr. & Meth **A393** (1997) 525.

[37] B. Girolami et al. Phys. Med. Bio. **41** (1996) 1581.

[38] K.J. Weeks, Nucl. Instr. & Meth. **A393** (1997) 544.

[39] V.N. Litvinenko et al. Phys. Rev. Lett. **24** (1997) 4569.

[40] A. Luccio and A.B. Brik, "Methods and Apparatus for Producing X-rays", US Patent 4,598,415 July 1 1986, European Patent 0,05032 24.08.1988.